

Electrocatalytic Response of Duplex and Yittria Dispersed Duplex Stainless Steel Modified Carbon Paste Electrode in Detecting Folic Acid Using Cyclic Voltammetry

R. Shashanka^{1,*}, D. Chaira¹, B.E. Kumara Swamy^{2,4}

¹Department of Metallurgical and Materials Engineering, National Institute of Technology Rourkela-769008, India

²Department of P.G .Studies and Research in Industrial Chemistry, Kuvempu University, Jnana Sahyadri, Shankaraghatta 577451, Shimoga, Karnataka, India.

*E-mail: shashankaic@gmail.com,

⁴E-mail: kumaraswamy21@gmail.com

Received: 5 February 2015 / Accepted: 21 March 2015 / Published: 27 May 2015

Duplex stainless steel of elemental composition Fe-18Cr-13Ni was mechanically alloyed in dual drive planetary ball mill for 10h. Milled powder sample was characterized by X-Ray diffraction, scanning electron microscope and high resolution electron microscope to study the morphology, lattice spacing and phases formed after milling for 10h. Then 1wt% Y₂O₃ nano particles were dispersed in duplex stainless steel powder by mixing the composition for 2h in turbula mixer. Carbon paste electrode was modified with yittria free and yittria dispersed duplex stainless steel respectively to study their electrocatalytic behavior in detecting folic acid. We determined optimum concentration of both the modifiers which show maximum anodic peak current in determining the folic acid. Among all, 8mg Yittria dispersed duplex stainless steel modified carbon paste electrode showed maximum current sensitivity than 4mg yittria free duplex stainless steel modified carbon paste electrode in 2mM folic acid concentration and 0.2M phosphate buffer solution of pH 7.2 at scan rate 100mVs⁻¹. We reported the effect of scan rate, concentration of folic acid and pH effect on oxidation peak of folic acid in both the modified carbon electrodes. Plot of all the above effects shows linear relationship and their electrode reactions were adsorption controlled. We successfully fabricated reliable, stable and fast response electrochemical sensor to detect folic acid.

Keywords: Yittria dispersed duplex stainless steel; electrocatalyst; cyclic voltammetry; folic acid; carbon paste:

1. INTRODUCTION

From past many years stainless steel became one of the basic materials in many industries due to their high strength, high corrosion resistance, high toughness, weldability, low thermal expansion

etc [1]. Duplex stainless steel is one of the types of stainless steel composed of both austenite and ferrite phases in almost same proportions [2, 3]. Some of the important applications of duplex stainless steel are chemical, oil, petrochemical, marine, nuclear power, paper and pulp industries [4-6]. In this paper duplex stainless steel was used as an electro chemical sensor to detect folic acid. No literature is available so far to use duplex stainless steel powder as a modifier to determine bioactive materials like folic acid (FA).

Due to the significant biological importance, the electro active material FA was selected as an analyte to study the electrochemical response [7]. FA is a part of vitamin B complex usually found in enriched foods, vitamin pills and employed in the treatment of megaloblastic anaemia during pregnancy, childhood, stroke, ischaemic heart disease [8] or colorectal cancer [9] and liver diseases [10]. Deficiency of FA causes gigantocytic anaemia, associated with leukopaenia, devolution of mentality, psychosis, etc [11]. Some of the common methods used to determine FA are ELISA (enzyme-linked immunosorbent assays) [12], capillary electrophoresis [13], high performance liquid chromatography with UV [14, 15] or diode array detection [16], microemulsion electrokinetic chromatography [17], spectrophotometry after coupling reaction with specific compounds [18], liquid chromatography with tandem mass spectroscopy [19] or with electro spray ionization mass spectrometry [20], biosensor-based determination [21]. Among all, cyclic voltammetric determination of FA gaining more attention in analysing electrochemical response of FA due to the low cost method, maximum sensitivity and more accurate measurements [22].

Some of the researchers used mercury electrode (Dropping mercury electrode) [23], mercury meniscus modified silver solid amalgam electrode (m-AgSAE) [24] and calixarene [22] as working electrodes to study the electrochemical response of FA. They reported maximum current sensitivity in acetate buffer at pH 5.5 with DME and fixed optimum condition of 9:1 aqueous acetate buffer and methanol mixture to detect nano molar FA concentration in pharmaceutical compounds.

Now a day, modified carbon paste electrodes become more advantageous than other electrodes due to clean and new surface availability during electrode reaction and extended potential window beyond +1.5V. Consolidating various suitable modifiers in carbon paste matrix made the electrode more sensitive, selective and robust in determining FA [22, 25-27]. Therefore, we used duplex and yttria dispersed duplex stainless steel powder samples as modifiers to detect electrochemical behaviour of FA.

Nanostructured duplex stainless steel powder was synthesized by high energy dual drive planetary ball mill (DDPM) and the details of milling parameters, mill fabrication were explained in our previous paper [28]. The duplex stainless steel powder was mixed uniformly with 1wt% of Y_2O_3 nano particles in a turbula mixer for 2h to get yttria dispersed duplex stainless steel powder. Due to the crystallographic stability at higher temperature, high thermal conductance and its structural stability with graphite even at 1600°C made Y_2O_3 to attract the attention of researchers [29]. Y_2O_3 dispersion in duplex stainless steel improves the surface properties of electrode by imparting stronger covalent bond and this result in the free movement of electrons between carbon paste and electrolytes [30]. Hence we fabricated duplex stainless steel modified carbon paste electrode (DMCPE) and yttria dispersed duplex stainless steel modified carbon paste electrode (YDMCPE) to study their electrocatalytic response in determining the FA using cyclic voltammetry. Electrocatalytic behaviour

of DMCPE and YDMCPE was compared successfully for 2mM folic acid in 0.2M phosphate buffer solution of pH 7.2 at a scan rate of 100mVs^{-1} . YDMCPE was found to be more selective, better, highly sensitive and anti material fouling electrode compared with DMCPE.

2. EXPERIMENTAL PART

2.1. Reagents and chemicals

Fe (99.5% pure), Cr (99.8% pure) and Ni (99.5% pure) elemental powders were purchased from loba chemicals. Folic acid, sodium dihydrogen ortho phosphate dihydrate and di-sodium hydrogen phosphate anhydrous of analytical grade quality was purchased from sd. Fine chemicals. All the above reagent solutions were prepared in double distilled water. Graphite powder was purchased from Merck chemicals.

2.2. Apparatus

DDPM was used to prepare nanostructured duplex stainless steel powder from the elemental powders of Fe, Cr and Ni. Final hour milled duplex stainless steel powders were characterized by X-ray diffraction (XRD) in a Philips PANalytical diffractometer using filtered Cu $K\alpha$ -radiation ($\lambda = 0.1542\text{ nm}$) to study the phases present in the stainless steel. Powder morphology was investigated by scanning electron microscopy (SEM) using JEOL JSM-6480LV. TEM microstructure, diffraction pattern and lattice spacing was investigated by using JEOL JEM-2100. Turbula mixer was used to disperse 1wt% Y_2O_3 nano particles in duplex stainless steel powder. Electrochemical work station CHI-660c model was used to investigate electrochemical measurements. The electrochemical cell composed of working electrode (carbon paste electrode of 3mm diameter), a platinum wire as counter electrode and Ag/AgCl saturated KCl electrode as reference electrode. The pH of the phosphate buffer solutions were measured in digital pH meter MK VI.

2.3 Synthesis of Duplex stainless steel powders by DDPM

The detailed synthesis and mill fabrication part was explained elsewhere [28] by the author.

2.4 Fabrication of the carbon paste electrode

Graphite powder and silicone oil at a ratio of 70:30 were taken in agate mortar and were hand mixed for 30min to prepare carbon paste electrode [31]. The cavity of working electrode was filled with prepared homogeneous carbon paste. The DMCPE was prepared by mixing duplex stainless steel powder along with graphite powder and silicone oil. Similarly, YDMCPE was prepared by homogeneous mixing of yttria dispersed duplex stainless steel powder, graphite powder and silicone

oil in agate mortar. The bare carbon paste electrode (BCPE) was prepared by mixing graphite powder and silicone oil but without modifier. The electrode surface was smoothed by rubbing the surface slowly on a piece of butter paper. The tube end of working electrode contains carbon paste and was electrically connected with copper wire.

3. RESULTS AND DISCUSSION

3.1 X-Ray Diffraction study

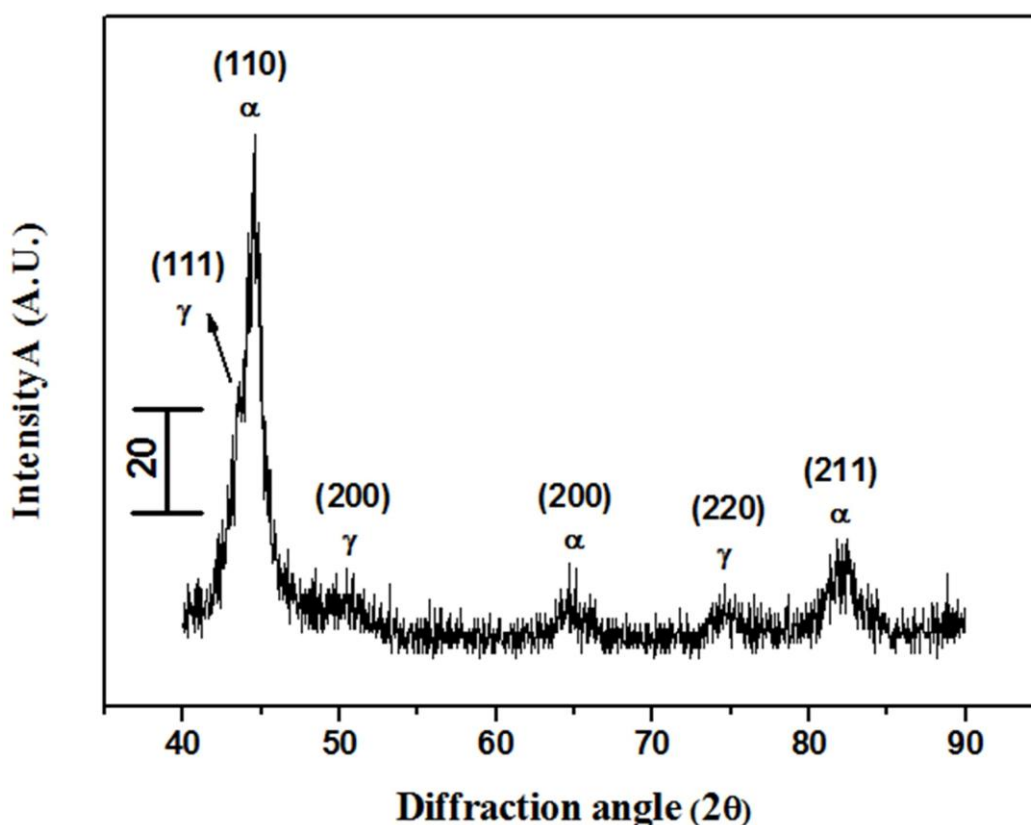


Figure 1. XRD spectrum of Fe-18Cr-13Ni (duplex stainless steel composition) milled for 10h in DDPM

Fig. 1 represents the XRD spectrum of duplex stainless steel (Fe-18Cr-13Ni) prepared in dual drive planetary mill for 10h. Usually milled powder associated with maximum internal strain, more defects and refined grain size due to the active collision of jar-powder-balls continuously. XRD spectra show broadened diffraction peaks due to the refined crystallite size and increased lattice strain during milling. Lattice parameter value for 10h milled duplex stainless steel was calculated by Nelson-Riley extrapolation method [32] and value was found to be 3.51\AA (matches with standard value 3.515\AA). Crystallite size and lattice strain of duplex stainless steel is calculated by Williamson-Hall method [3] and they are found to be 8nm and 5.595×10^{-3} respectively. Grain boundary volume fractions increases due to the process of grain size reduction, structural defect and amorphization during milling. This

results in formation of more defect storage sites, shorter diffusion path and attains meta-stable non-equilibrium state during milling [28].

3.2 Microstructure study

3.2.1 Scanning electron microscopy (SEM)

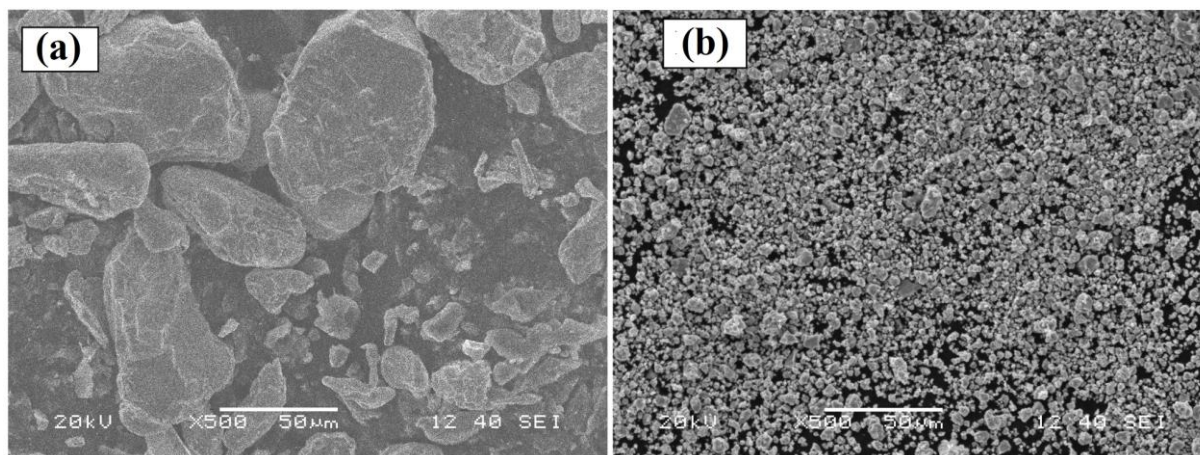


Figure 2. SEM micrographs of duplex stainless steel powder milled for (a) 0h (b) 10h in DDPM

Fig. 2 (a) and 2 (b) represents the SEM images duplex stainless steel powder milled for 0h and 10h respectively. At 0h (before milling) elemental powder samples are large and random in size but after 10h of milling particles become spherical and very small. During milling, the powder particles becomes flat plate like structures due to the presence of ductile iron and two or more plate like structure weld together to form giant structure after few hours of milling. Further increase in milling time results in the work hardening and fragments in to very fine regular, uniform and spherical duplex stainless steel powders. Due to very fine particle morphology the surface area and surface energy of the particles increases. Therefore we studied the electrocatalytic properties of duplex stainless steel powders.

3.2.2 High resolution transmission electron microscopy (HRTEM)

The HRTEM microstructure, selected area electron diffraction pattern (SAED) and lattice spacing of 10h milled duplex stainless steel powder sample is shown in the fig. 3 (a), 3 (b) and 3 (c) respectively. Fig. 3 (a) depicts the bright field image of duplex stainless steel crystallites with size around 30nm each. Due to their nano size the surface area, surface energy and reactivity increases, hence particles looks agglomerate as shown in the figure. As we know that duplex is a combination of almost equal proportions of both austenite and ferrite phases. Therefore we investigated the phases present in duplex stainless steel by SAED method as shown in the fig. 3 (b). Different crystallographic planes were indexed and it confirms the presence of both ferrite and austenite phases. The SAED

pattern contains airy ring structures with few spotty appearances, which confirms the formation of nanostructured duplex stainless steel after 10h of milling. Fig. 3 (c) shows the HRTEM image of lattice spacing of planes present in duplex stainless steel is found to be 2.105\AA . Therefore lattice parameter value of austenite phase in duplex stainless steel is 3.64\AA and that of ferrite phase is 2.97\AA respectively.

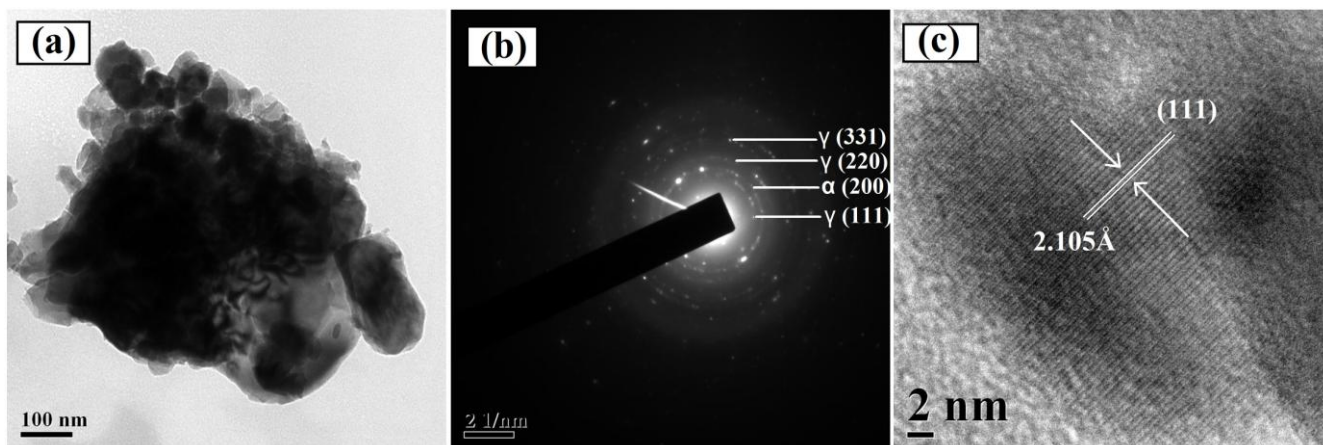


Figure 3. TEM images of duplex stainless steel powder (a) Bright field TEM image (b) SAED pattern (c) HRTEM lattice spacing image

3.3. Electrocatalytic response of FA at DMCPE

3.3.1 Concentration variation of nanostructured duplex stainless steel powder

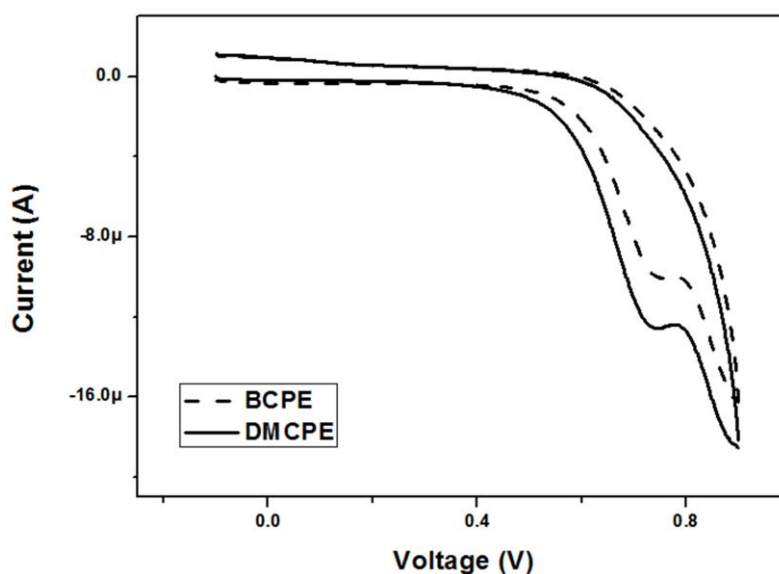


Figure 4. Cyclic voltammogram of bare carbon paste electrode (BCPE) and 4mg DMCPE in 2mM FA at 100mVs^{-1} and in PBS of pH 7.2

Concentration of the modifier plays an important role in increasing the efficiency, surface area, selectivity and sensitivity of the electrode. Therefore, we studied the electrochemical response of FA at different concentration of duplex stainless steel. The concentration of the modifier was varied from 2, 4, 6, 8mg and investigated anodic peak current of 2mM FA in 0.2M phosphate buffer of pH 7.2 at scan rate of 100mVs^{-1} . The main purpose of using a modifier is to increase the peak current and decreases the over potential for the redox reactions. DMCPE with 4mg concentration of duplex stainless steel show maximum anodic peak current and hence 4mg DMCPE was selected as the electrode for further electrochemical study of 2mM FA. Fig. 4 represents the cyclic voltammogram of BCPE and 4mg DMCPE. The dotted curve and straight line curve represents the cyclic voltammogram of 2mM FA at BCPE and DMCPE respectively. The anodic peak current at BCPE is less sensitive when compared to DMCPE.

3.3.2 Effect of scan rate on the anodic peak current of FA

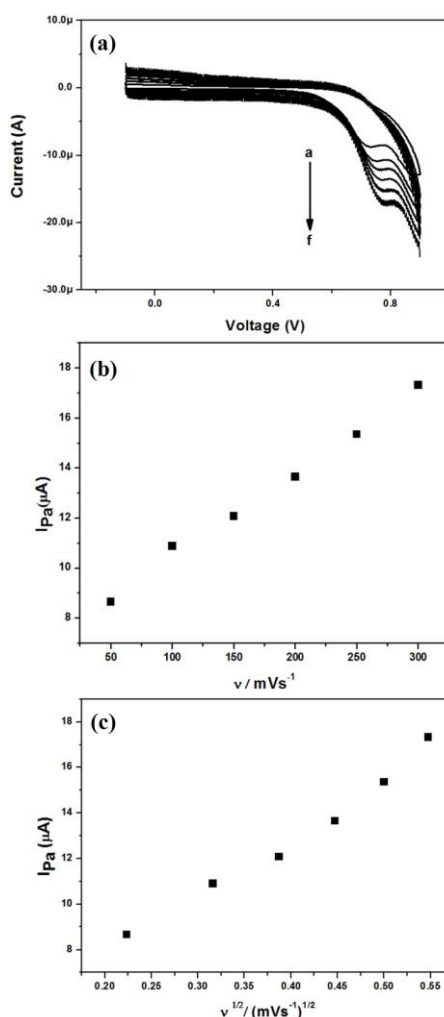


Figure 5. (a) Cyclic voltammogram of 2mM FA using 4mg DMCPE at 50 to 300mVs^{-1} scan rate ($a=50, b=100, \dots, f=300\text{mVs}^{-1}$) in PBS of pH 7.2 (b) Plot of anodic peak current vs. scan rate (c) Plot of anodic peak current vs. square root of scan rate

Kinetic studies of electrode reactions can be investigated by varying the scan rates; hence scan rate effect is a very important parameter used to study the stability of the electrode. The effect of scan rate was performed by increasing the scan rate from 50 to 300mVs⁻¹ for 2mM FA in phosphate buffer solution (PBS) of pH 7.2. Cyclic voltammogram of 2mM FA in 4mg DMCPE at different scan rates was shown in fig. 5 (a). The oxidation peak current and anodic peak potential increases linearly with increase in the scan rate from 50 to 300mVs⁻¹. The oxidation peak current at 50mVs⁻¹ is found to be 8.67μA and at 300mVs⁻¹ is 17.32μA respectively. Fig. 5 (b) shows the plot of anodic peak current vs. different scan rate. The anodic peak current increase linearly with correlation coefficient is 0.9931. Hence this indicates that the electrode process is diffusion controlled [33]. The anodic peak current vs. square root of scan rate is shown in fig. 5 (c) and their correlation coefficient is found to be 0.9880.

3.3.3 Effect of Concentration of folic acid

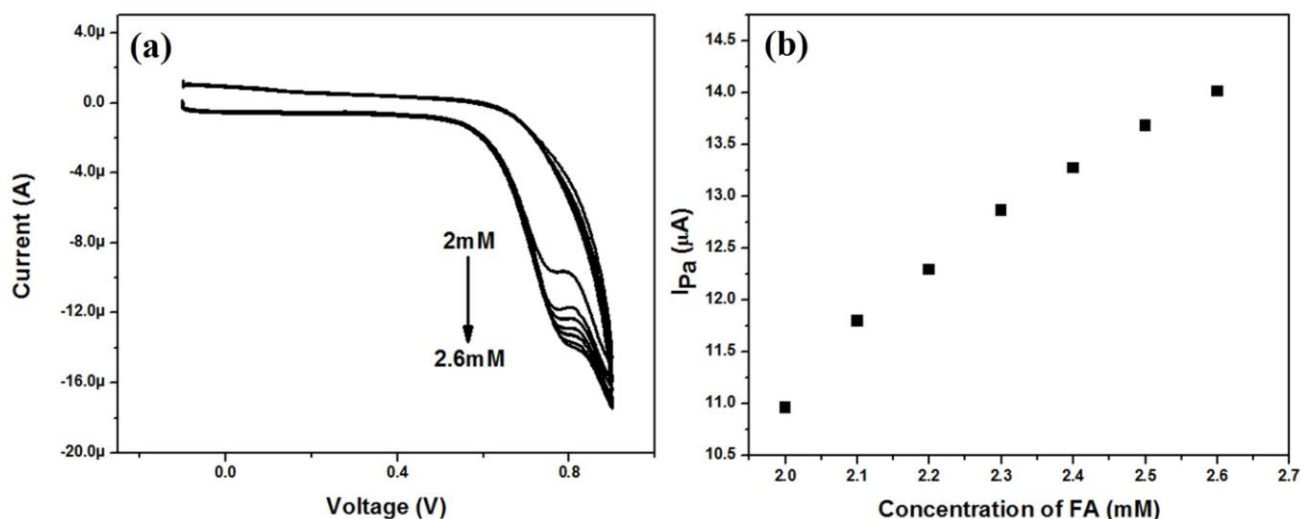


Figure 6. (a) Cyclic voltammogram of 2 to 2.6mM concentration of FA at 100mVs⁻¹ in PBS of pH 7.2 using 4mg DMCPE (b) Plot of anodic peak current vs. different concentration of FA

Electrocatalytic behaviour of 4mg DMCPE was studied by varying the concentrations of FA.

In general, the anodic peak current increases with increase in the concentration of analyte. Fig. 6 (a) depicts the cyclic voltammogram of FA at 2 to 2.6mM concentration at phosphate buffer solution (PBS) of pH 7.2 and scan rate of 100mVs⁻¹. From the fig it is evident that, as the concentration of FA increases from 2 to 2.6mM then anodic peak current also increases along with anodic peak potential. Anodic peak potential at 2mM FA is found to be 768mV and at 2.6mM FA is 812mV respectively. Fig. 6 (b) depicts the plot of anodic peak current vs. different concentration of FA. Plot shows the linear relationship between anodic peak current and different concentration of FA with correlation coefficient of 0.9757. The anodic peak current at 2mM FA is 10.96μA and at 2.6mM FA concentration it has been increased to 14.01μA. The increase in peak current is due to the availability of more FA molecules at higher concentration, hence more number of electrons involved in electrode reactions.

Ardakani et al. [34] investigated the effect of concentration of FA by nanostructured mesoporous material modified carbon paste electrode and reported the similar kind of results.

3.3.4 Effect of pH

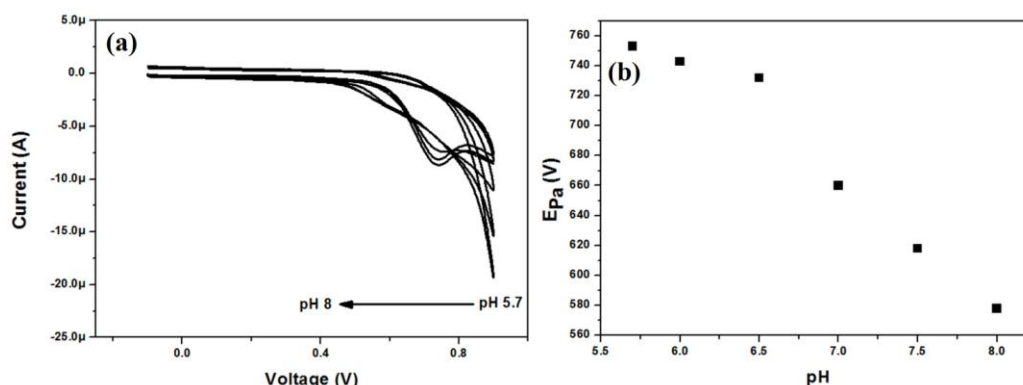


Figure 7. (a) Cyclic voltammogram of 2mM FA at different pH of PBS buffer solutions at 100mVs⁻¹ using 4mg DMCPE (b) Plot of anodic peak current vs. different pH from values 5.7 to 8

The electrocatalytic response of 4mg DMCPE in 2mM FA at different pH of PBS was studied successfully. Generally redox potential shift towards the lower potential side at higher pH. Fig. 7 (a) depicts the cyclic voltammogram of 2mM FA at different pH from 5.7 to 8. From the voltammogram it is evident that the oxidation peak potentials of 2mM FA were shifted towards a lower potential side with the increase of pH value. Because, FA undergoes oxidation very easily at higher pH values, higher the pH value higher will be the oxidation rate of FA. Fig. 7 (b) represents the plot of different pH vs. anodic peak potential of 2mM FA at scan rate of 100mVs⁻¹. The Anodic peak potential decreases linearly from pH 5.7 to 8 with correlation coefficient of 0.9487. The oxidation peak potential at pH 5.7 is 753mV and at pH 8 it is decreased to 578mV respectively. Arvand and Dehsaraei [35] studied the effect of scan rate, effect of concentration of FA and effect of pH on the gold nanoparticles modified carbon paste electrode and reported similar kind of results.

3.4. Electrocatalytic response of FA at YDMCPE

3.4.1 Concentration variation of nanostructured duplex stainless steel powder

Electrocatalytic behavior of YDMCPE at different concentration of yttria dispersed duplex stainless steel modifier was studied successfully. Modifiers play very important role in increasing the peak current and there by decreases the over potential of the redox reactions.

The concentration of yttria dispersed stainless steel powder was varied from 2, 4, 6, 8, 10 and 12mg respectively and measured their anodic peak current at 2mM FA in 0.2M phosphate buffer of pH 7.2 at scan rate of 100mVs⁻¹. YDMCPE with 8mg yttria dispersed duplex stainless steel show

maximum oxidation peak current and hence it was selected as the electrode for further electrochemical study of 2mM FA. We reported the effect of scan rate, effect of concentration and effect of pH on the anodic peak. Fig. 8 depicts the cyclic voltammogram of BCPE and 8mg YDMCPE. The oxidation peak current of 8mg YDMCPE at 2mM FA shows maximum current sensitivity than BCPE and 4mg DMCPE. The anodic peak current of BCPE is $10\mu\text{A}$, DMCPE is $12.60\mu\text{A}$ and YDMCPE is $15.87\mu\text{A}$ respectively.

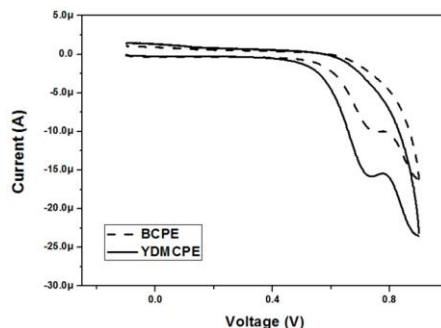


Figure 8. Cyclic voltammogram of bare carbon paste electrode (BCPE) and 8mg YDMCPE in 2mM FA at 100mVs^{-1} and in PBS of pH 7.2

3.4.2 Effect of scan rate

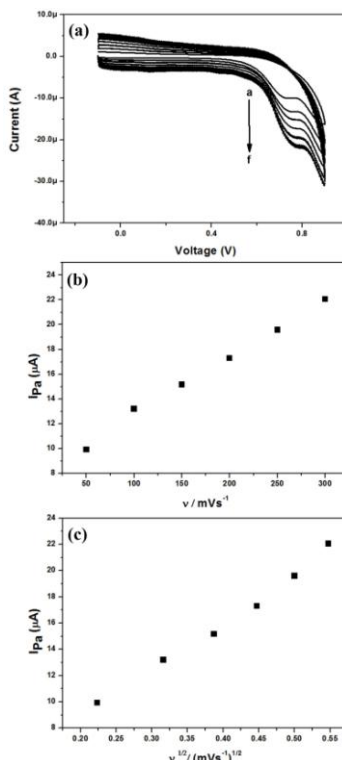


Figure 9. (a) Cyclic voltammogram of 2mM FA using 8mg YDMCPE at 50 to 300mVs^{-1} scan rate (a=50, b=100,, f= 300mVs^{-1}) in PBS of pH 7.2 (b) Plot of anodic peak current vs. scan rate (c) Plot of anodic peak current vs. square root of scan rate

Fig. 9 (a) shows the cyclic voltammogram of 2mM FA at a scan rate of 50 to 300mVs⁻¹ in PBS of pH 7.2. From the fig it is confirmed that both anodic peak current and potential increases with increase in scan rate. The anodic peak potential increases from 724 to 780mV at 50 to 300mVs⁻¹ respectively. Fig 9 (b) depicts the plot of scan rate vs. anodic peak current of 2mM FA at 100mVs⁻¹ in PBS of pH 7.2 and it varies from 9.92μA at 50mVs⁻¹ to 22.05μA at 300mVs⁻¹ respectively. The correlation coefficient of the plot is 0.9937 and this reveals that electrode process is diffusion controlled [35]. Similarly, fig. 9 (c) represents the plot of square root of scan rate vs. anodic peak current of 2mM FA and the correlation coefficient is found to be 0.9749.

3.4.3 Effect of Concentration of Folic acid

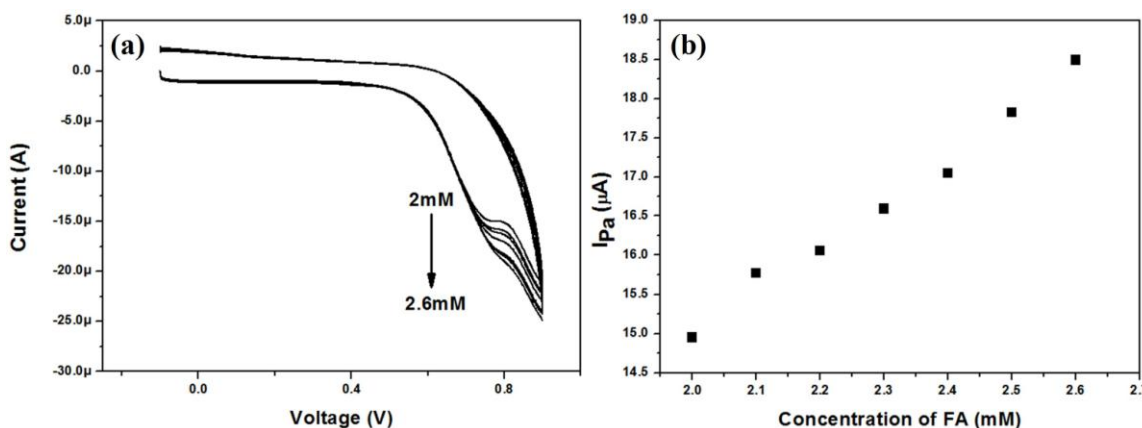


Figure 10. (a) Cyclic voltammogram of 2 to 2.6mM concentration of FA at 100mVs⁻¹ in PBS of pH 7.2 using 8mg YDMCPE (b) Plot of anodic peak current vs. different concentration of FA

The anodic peak current of FA increases linearly with increase in the concentration of FA in an electrochemical cell. Fig. 10 (a) represents the cyclic voltammogram of 8mg YDMCPE at 2 to 2.6mM FA concentration. From the voltammogram it is confirmed that anodic peak potential increase linearly with increase in concentration of FA. The oxidation potential increases from 764 to 778mV at 2mM to 2.6mM FA concentrations. Fig. 10 (b) shows the plot of anodic peak current vs. different concentration of FA and it shows linear relationship with correlation coefficient of 0.9850. The anodic peak current increases from 14.95μA to 18.49μA at 2mM to 2.6mM FA concentrations. Baghbamidi et al. [36] studied the effect of concentration of FA from 0.1 to 700μM using modified carbon paste electrode. They reported the linear increase in the peak current with increase in the concentration of FA.

3.4.4 Effect of pH

It is very important to know the optimum pH value at which the electrodes show maximum sensitivity, selectivity and less material fouling during electrochemical measurements. Therefore, we studied the electrochemical response of YDMCPE at pH 5.7 to 8 using 2mM FA at a scan rate of 100mVs⁻¹. Fig. 11 (a) represents the voltammogram of 2mM FA at different pH values of 0.2M PBS.

The anodic peak potentials of 2mM FA were shifted towards lower potential side with the increase of pH value as show in the voltammogram. This is due to the higher oxidation rate of FA at higher pH values. Fig. 11 (b) represents the plot of different pH values vs. anodic peak potential of FA. Oxidation peak potential of FA decreases linearly from pH 5.7 to 8 with correlation coefficient of 0.9407 as shown in the plot. At pH 5.7 the oxidation peak potential is 757mV and at pH 8 it is decreased to 550mV respectively.

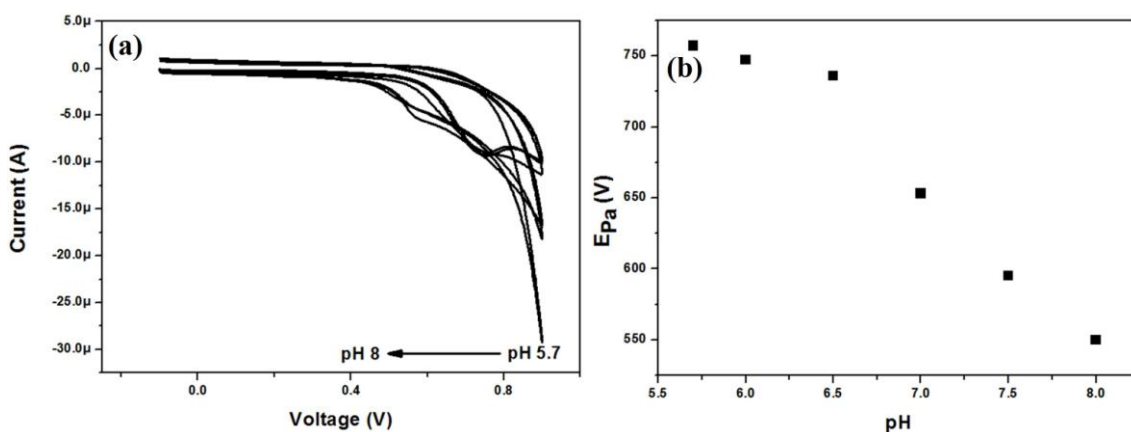


Figure 11. (a) Cyclic voltammogram of 2mM FA at different pH of PBS buffer solutions at 100mVs⁻¹ using 8mg YDMCPE (b) Plot of anodic peak current vs. different pH from values 5.7 to 8

4. CONCLUSION

Duplex stainless steel powder was prepared by milling elemental powders of Fe, Cr and Ni in DDPM for 10h. The effect of milling on particle morphology was explained by the author in previous paper [28]. Successfully fabricate the DMCPE and YDMCPE to study electrochemical behaviour of FA. YDMCPE show strong electrocatalytic activity towards the oxidation of FA than DMCPE. High selectivity, low cost and high sensitivity of the electrocatalytic response of DMCPE and YDMCPE made them very useful sensors in determining FA. Both the electrodes can be used as sensor in medical field for the diagnosis of FA deficiency diseases. Almost all the electrode reactions at the above bioactive compounds are adsorption controlled reactions.

ACKNOWLEDGEMENTS

Financial support for this work from the Council of Scientific & Industrial Research (CSIR), India (Grant No. 22/561/11/EMR II Dated 11.04.2011) is gratefully acknowledged.

References

1. D.P. Selvaraj, P. Chandramohan, M. Mohanraj, *Measurement*. 49 (2014) 205–215.
2. L.A. Dobrzanski, Z. Brytan, M. Actis Grande, M. Rosso, *Archives of Materials Science and Engineering*. 28 (2007) 217–223.

3. R. Shashanka, D. Chaira, *Mater Charact.* 99 (2015) 220–229.
4. S. Herenu, I. Alvarez-Armas, A.F. Armas, *Scripta Mater.* 45 (2001) 739–745.
5. H. Miyamoto, T. Mirnaki, S. Hashimoto, *Mater Sci Eng A.* 319 (2001) 779–783.
6. M.J. Schofield, R. Bradsha, R.A. Cottis, *Mater Performance.* 35 (2009) 65–70.
7. A.L. Lehninger, *Principles of Biochemistry*, Worth, New York, (1982).
8. D.S. Wald, N.J. Wald, J.K. Morris, M. Law, *BMJ.* 333 (2006) 1114–1117.
9. C. La Vecchia, E. Negri, C. Pelucchi, S. Franceschi, *Int. J. Cancer.* 102 (2002) 545–547.
10. F.J. Al-Shammary, K.A. Al-Rashood, N.A. Mian, M.S. Mian, *Anal Profiles Drug Sub.* 19 (1990) 221.
11. H.X. Guo, Y.Q. Li, L.F. Fan, X.Q. Wu, M.D. Guo, *Electrochim Acta.* 51 (2006) 6230–6237.
12. J. Alaburda, A.P. De Almeida, L. Shundo, V. Ruvieri, M. Sabino, *J Food Comp Anal.* 21 (2008) 336–342.
13. S.L. Zhaoa, H.Y. Yuan, C. Xie, D. Xiao, *J Chromatogr A.* 1107 (2006) 290–293.
14. L.A. Kozhanova, G.A. Fedorova, G.I. Baram, *J Anal Chem.* 57 (2002) 40–45.
15. U. Holler, C. Brodhag, A. Knobel, P. Hofmann, V. Spitzer, *J Pharm Biomed Anal.* 31 (2003) 151–158.
16. H.B. Li, F. Chen, *J Sep Sci.* 24 (2001) 271–274.
17. R.H.F. Cheung, J.G. Hughes, P.J. Marriott, D.M. Small, *Food Chem.* 112 (2009) 507–514.
18. P. Nagaraja, H.R. Arun kumar, R.A. Vasantha, H.S. Yathirajan, *Anal. Biochem.* 307 (2002) 316–321.
19. M. Rychlik, S. Monch, *Ernahr. –Umsch.* 56 (2009) 270–273.
20. J.D.M. Patring, J.A. Jastrebova, *J Chromatogr A.* 1143 (2007) 72–82.
21. M.B. Caselunghe, J. Lindeberg, *Food Chem.* 70 (2000) 523–532.
22. V.D. Vaze, A.K. Srivastava, *Electrochim Acta.* 53 (2007) 1713–1721.
23. E. Jacobsen, M.W. Bjornsem, *Anal Chim Acta.* 96 (1978) 345–351.
24. L. Bandzuchova, R. Selesovska, T. Navratil, J. Chylkova, *Electrochim Acta.* 56 (2011) 2411–2419.
25. B.E. Conway, R.G. Barradas, *Electrochim Acta.* 5 (1961) 319–348.
26. P. Valenta, H.W. Nurnberg, D. Krznaric, *Bioelectrochem Bioenerg.* 3 (1976) 418–439.
27. C. Samiha, B. Ender, C. Osman, *J Inorg Biochem.* 77 (1999) 249–255.
28. R. Shashanka, D. Chaira, *Powder Technol.* 259 (2014) 125–136.
29. P.V.A. Padmanabhan, S. Ramanathan, K.P. Sreekumar, R.U. Satpute, *Mater Chem Phys.* 106 (2007) 416–421.
30. C.A. Traina, J. Schwartz, *Langmuir.* 23 (2007) 9158–9161.
31. R. Shashanka, B.E.K. Swamy, S. Reddy, D. Chaira, *Anal Bioanal Electrochem.* 5 (2013) 455–466.
32. B.D. Cullity, S.R. Stock, *Elements of X-Ray Diffraction*, Pearson, (2003). (Paperback, ISBN-13: 9780131788183).
33. Mohammad Mazloum-Ardakani, Fariba Sabaghian, Alireza Khoshroo, Hossein Naeimi, *Chinese J Catal.* 35 (2014) 565–572.
34. Mohammad Mazloum-Ardakani, Mohammad Ali Sheikh-Mohseni, Mohammad Abdollahi-Alibeik, Ali Benvidi, *Sensor Actuat B.* 171–172 (2012) 380–386.
35. Majid Arvand, Mohammad Dehsaraei, *Mater Sci Eng C.* 33 (2013) 3474–3480.
36. Sakineh Esfandiari Baghbamidi, Hadi Beitollahi, Hassan Karimi-Maleh, Somayeh Soltani-Nejad, Vahhab Soltani-Nejad, Sara Roodsaz, *Journal of Analytical Methods in Chemistry*, 2012 (2012) 1–8.